Criticality in the duration of quasistationary state

Antonio Rodríguez,[1] Fernando D. Nobre,[2] and Constantino Tsallis[2,3,4]

[1]*GISC, Departamento de Matemática Aplicada a la Ingeniería Aeroespacial, Universidad Politécnica de Madrid, Plaza Cardenal Cisneros s/n, 28040 Madrid, Spain*

[2]*Centro Brasileiro de Pesquisas Físicas and National Institute of Science and Technology for Complex Systems, Rua Dr. Xavier Sigaud 150, 22290-180, Rio de Janeiro, Brazil*

[3]*Santa Fe Institute, 1399 Hyde Park Road, Santa Fe, New Mexico 87501, USA*

[4]*Complexity Science Hub Vienna, Josefstädter Strasse 39, 1080 Vienna, Austria*

(Received 4 May 2021; accepted 13 July 2021; published 29 July 2021)

The duration of the quasistationary states (QSSs) emerging in the d-dimensional classical inertial α-XY model, i.e., N planar rotators whose interactions decay with the distance r_{ij} as $1/r_{ij}^{\alpha}$ ($\alpha \geqslant 0$), is studied through first-principles molecular dynamics. These QSSs appear along the whole long-range interaction regime ($0 \leqslant \alpha/d \leqslant 1$), for an average energy per rotator $U < U_c$ ($U_c = 3/4$), and they do not exist for $U > U_c$. They are characterized by a kinetic temperature $T_{\rm QSS}$, before a crossover to a second plateau occurring at the Boltzmann-Gibbs temperature $T_{\rm BG} > T_{\rm QSS}$. We investigate here the behavior of their duration $t_{\rm QSS}$ when U approaches U_c from below, for large values of N. Contrary to the usual belief that the QSS merely disappears as $U \to U_c$, we show that its duration goes through a critical phenomenon, namely $t_{\rm QSS} \propto (U_c - U)^{-\xi}$. Universality is found for the critical exponent $\xi \simeq 5/3$ throughout the whole long-range interaction regime.

DOI: 10.1103/PhysRevE.104.014144

I. INTRODUCTION

Critical phenomena appear frequently, mostly resulting from a collective behavior in many-component systems, which exhibit large instabilities and fluctuations near criticality [1–5]. They are found in various areas, from social to natural sciences, in equilibrium and nonequilibrium regimes, being characterized by significant alterations in their associated fundamental properties; as typical examples one may mention earthquakes, strong climate changes, stock-market crashes, and phase transitions. The latter ones, particularly equilibrium phase transitions occurring in fluids and magnetic systems, have been extensively studied in the literature [1,2]. As a prototype, one has the simple ferromagnet, where a well-defined critical point typified by a temperature T_c (or equivalently, by a critical internal energy per particle U_c) signals a continuous phase transition between paramagnetic and ferromagnetic states. Continuous equilibrium phase transitions are characterized by a significant increase of correlations, leading to a powerlike divergence of the correlation length at criticality; consequently, power-law behavior emerges in the divergence of response functions, as well as in the onset of associated order parameters. A peculiar situation occurs in the two-dimensional XY model, where a Kosterlitz-Thouless ordering (usually known as a soft phase) presents a divergent correlation length for all $T \leqslant T_{\rm KT}$ [2].

Nonequilibrium regimes are very common in nature, so that a diversity of nonequilibrium critical phenomena has also been found (see, e.g., Refs. [4,5]), some of them being specified by critical parameters, whereas in other cases the fine tuning of certain quantities is not necessary. Herein we present a critical phenomenon that occurs in a quasistationary state (QSS) of a system of XY rotators interacting through long-distance ferromagnetic couplings. For given values of the internal energy per rotator U, we will show numerical evidence that the duration of the QSS (hereafter denoted $t_{\rm QSS}$) increases with U approaching U_c, exhibiting a power-law divergence as $U \to U_c$ from below, where U_c denotes the critical energy per particle, to be defined below.

II. THE $\alpha - XY$ INERTIAL MODEL

Apart from its potential-energy contribution, the system we analyze herein presents also a kinetic term in the Hamiltonian, enabling equations of motion to be derived. More precisely, the so-called α-XY inertial model is defined by the Hamiltonian [6]

$$\mathcal{H} = K + V_\alpha = \sum_{i=1}^{N} E_i,$$

$$E_i = \frac{p_i^2}{2} + \frac{1}{2\widetilde{N}} \sum_{j \neq i}^{N} \frac{1 - \cos(\theta_i - \theta_j)}{r_{ij}^{\alpha}}, \qquad (1)$$

where, from now on, without loss of generality, we set moments of inertia, coupling constants, as well as $k_{\rm B}$, equal to the unit. The model consists of N two-component rotators (with length normalized to the unit), located at the sites of a d-dimensional hypercubic lattice of linear size L ($N \equiv L^d$) and the ferromagnetic interactions between pairs decay with their respective distance $r_{ij} = |\mathbf{r}_i - \mathbf{r}_j|$ (measured in lattice units and defined as the minimal one, since periodic conditions will be used). Moreover, the parameter $\alpha \geqslant 0$ controls the interaction range, interpolating between two special limits,

namely, $\alpha = 0$ and $\alpha \to \infty$, corresponding respectively to the Hamiltonian mean-field (HMF) model [7], characterized by fully coupled planar rotators, and to nearest-neighbor-interaction models. The two time-dependent contributions, $K \equiv K(t)$ and $V_\alpha \equiv V_\alpha(t)$, represent the kinetic and potential energies at time t, whereas $E_i \equiv E_i(t)$ stands for one-particle energies; these quantities follow the conservation of total energy, i.e., $\mathcal{H} = K(t) + V_\alpha(t) = \sum_i E_i(t) = \text{const}$ $(\forall t)$. Furthermore, the prefactor in the potential energy of Hamiltonian (1) yields an "extensive" energy for all values of α/d, where [8,9]

$$\widetilde{N} = \frac{1}{N} \sum_{i=1}^{N} \sum_{j \neq i}^{N} \frac{1}{r_{ij}^{\alpha}} = \sum_{j=2}^{N} \frac{1}{r_{1j}^{\alpha}}, \tag{2}$$

recovering the expected quantities in the two special limits, i.e., $\widetilde{N} = N - 1 \sim N$ $(\alpha = 0)$ and $\widetilde{N} = 2d$ $(\alpha \to \infty)$.

The HMF model has been largely investigated in the literature (see, e.g., Refs. [7,10–19]), leading to many anomalous properties, such as negative specific heat, QSSs, non-Maxwellian velocity probability distributions, and ergodicity breaking, among others. Some of these features have been addressed through connections with the Vlasov equation (see, e.g., Refs. [20–24] and references therein), as well as within nonextensive statistical mechanics [25,26]. This framework emerged through the proposal of a generalized entropic form [27],

$$S_q = k \sum_{i=1}^{W} p_i \left(\ln_q \frac{1}{p_i} \right), \tag{3}$$

where $\ln_q u \equiv (u^{1-q} - 1)/(1-q)$ $(\ln_1 u = \ln u)$, being characterized by an index q $(q \in \mathbb{R})$, recovering Boltzmann-Gibbs (BG) entropy in the limit $q \to 1$, i.e., $S_1 \equiv S_{\text{BG}}$. As a consequence, the distributions that optimize the entropy S_q generalize the Gaussian into the usually referred to as q-Gaussian probability distributions [25,26].

A special interest was also dedicated to the α-XY model [cf. Eq. (1)], either on a ring (dimension $d = 1$) (see, e.g., Refs. [6,28–30]), or on d-dimensional lattices $(d = 1, 2, 3)$ [31–33]. By means of first-principles molecular-dynamics simulations, it was shown that the largest Lyapunov exponent scales with the total number of rotators as $N^{-\kappa}$, where κ depends on (α, d) only through the ratio α/d, leading to $\kappa > 0$ in the long-range regime $(0 \leqslant \alpha/d \leqslant 1)$, whereas $\kappa \to 0$ in the short-range regime $(\alpha/d > 1)$, corresponding to positive Lyapunov exponents. Moreover, q-Gaussian probability distributions have been obtained for the time-averaged momenta distributions, both before and after the transition to the long-standing state whose kinetic temperature coincides with that of the BG equilibrium state, with a value of the entropic index $q = q_p(\alpha/d)$ within the long-range regime [32]. On the other hand, Maxwellian distributions were found in the limiting short-range regime, as well as for ensemble-averaged momenta probability distributions. Deviations from BG predictions have also been observed for time-averaged energy probability distributions, where instead of the BG exponential, q-exponential probability distributions emerged from the simulations in the long-range regime, with $q = q_E(\alpha/d)$ [32]. Essentially similar results have been obtained for an analogous system, defined in terms of Heisenberg (three-component) classical rotators, usually called the inertial α-Heisenberg model [34–36], as well as for a long-range-interaction Fermi-Pasta-Ulam model [37–41].

The model defined in Eq. (1) will be studied numerically by molecular-dynamics simulations, i.e., by a direct integration of the equations of motion,

$$\dot{\theta}_i = \frac{\partial \mathcal{H}}{\partial p_i} = p_i, \quad \dot{p}_i = -\frac{\partial \mathcal{H}}{\partial \theta_i} = -\frac{1}{\widetilde{N}} \sum_{j \neq i}^{N} \frac{\sin(\theta_i - \theta_j)}{r_{ij}^{\alpha}}, \tag{4}$$

where the angle $\theta_i(t)$, together with its conjugated angular momentum $p_i(t)$, describe the state of rotator i $(i = 1, 2, \ldots, N)$ at time t. Two important quantities, namely, the kinetic temperature and internal energy per particle, are defined in the usual way,

$$T(t) = \frac{2}{N} \langle K(t) \rangle, \quad U \equiv \frac{\langle \mathcal{H} \rangle}{N} = \frac{1}{N} \sum_i \langle E_i(t) \rangle, \tag{5}$$

whereas a ferromagnetic order (whenever present) is characterized by the norm of the magnetization vector,

$$\vec{M}(t) = \frac{1}{N} \sum_{i=1}^{N} \vec{S}_i(t), \tag{6}$$

with $\vec{S}_i(t) \equiv [\cos\theta_i(t), \sin\theta_i(t)]$. In the HMF limit $(\alpha = 0)$ one gets from Eq. (1),

$$U = \frac{T}{2} + \frac{1}{2}(1 - M^2), \tag{7}$$

which, in fact, was shown to apply throughout the whole range $0 \leqslant \alpha/d \leqslant 1$ of the α-XY inertial model [28,29]. Therefore, this model presents a paramagnetic-ferromagnetic continuous phase transition at the critical values $T_c = 1/2$ and $U_c = 3/4$.

Previous investigations of the α-XY inertial model (see, e.g., Refs. [31,32]) have shown the existence of long-living QSSs for $0 \leqslant \alpha/d \leqslant 1$ and $U \lesssim U_c$. A particular emphasis was given to these QSSs for the energy value $U = 0.69$, showing a crossover to a state whose temperature coincides with the one obtained within BG statistical mechanics. Recently, detailed numerical analyses focused on the duration t_{QSS} for both α-XY $(U = 0.69)$ [33] and α-Heisenberg (for a given $U \lesssim U_c$, where $U_c = 5/6$) [36] inertial models. It was shown that t_{QSS} presents similar behavior for these two models, i.e., it depends on N, α, and d; in fact, t_{QSS} decreases with α/d and increases with both N and d [33,36].

III. QSS DURATION AS A FUNCTION OF U

In the present work we vary the internal energy per rotator U $(U \leqslant U_c)$ to investigate the U dependence of the duration t_{QSS} for the α-XY inertial model. The numerical procedure follows Ref. [33], i.e., the $2N$ equations in (4) were integrated by means of a fourth-order symplectic algorithm [42], considering an integration step $h = 0.2$, yielding conservation of the energy per particle within a relative precision of 10^{-4} (at least) throughout all our calculations. We applied periodic boundary conditions and a fast-Fourier-transform algorithm, for which the total number of rotators were chosen as $N = l^6 = (l^3)^2 =$

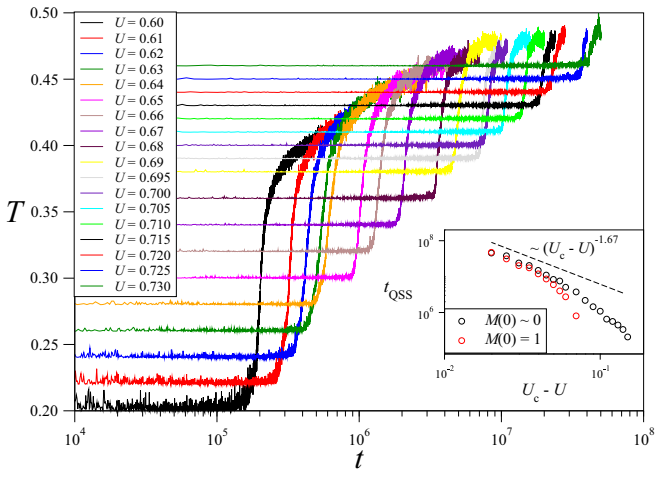

FIG. 1. The kinetic temperature $T(t)$ [cf. Eq. (5)] of the HMF model is represented vs time (in logarithmic scale), considering initial magnetization $M(0) \simeq 0$, different values of the internal energy per rotator $U < U_c$ ($U_c = 3/4$), and $N = 30\,000$. Notice that $t_{\rm QSS}$ grows with U, as U_c is approached from below. A similar analysis may be carried for the initial condition $M(0) = 1$ and the results for both conditions are compared in the inset, where the duration $t_{\rm QSS}$ is represented vs $(U_c - U)$ in a log-log plot. For this value of N, QSSs are identified clearly throughout different ranges of U, comparing the two initial conditions (see text).

$(l^2)^3$ ($l = 4, 5, 6, 7, 8, 9, 10$), all of them being expressed in the form $N = L^d$ ($d = 1, 2, 3$). Hence, we used $N = 4096 = (64)^2 = (16)^3$, $15\,625 = (125)^2 = (25)^3$, $46\,656 = (216)^2 = (36)^3$, $117\,649 = (343)^2 = (49)^3$, $262\,144 = (512)^2 = (64)^3$, $531\,441 = (729)^2 = (81)^3$, and $10^6 = (1000)^2 = (100)^3$. At the initial time, the angular momenta $\{p_i\}$ were drawn from a uniform distribution, $p_i \in [-1, 1]$, then rescaled to achieve the desired value for U and $\sum_i p_i = 0$. For the angles, we chose θ_i from a uniform distribution $\theta_i \in [0, 2\pi]$, as well as $\theta_i = 0\ (\forall i)$, corresponding to minimum ($M(0) \simeq 0$) and maximum ($M(0) = 1$) total magnetizations, respectively; as shown in Ref. [33], both initial conditions yielded qualitatively similar results for the duration $t_{\rm QSS}$.

In Fig. 1 we represent the kinetic temperature $T(t)$ of Eq. (5) in a linear-log plot, for an HMF model with $N = 30\,000$ rotators, initial magnetization $M(0) \simeq 0$, and several values of the internal energy per rotator $U < U_c$ ($U_c = 3/4$). A similar analysis may be carried for the initial condition $M(0) = 1$, where for this value of N, clear QSSs are identified in the energy range $0.68 \leqslant U \leqslant 0.73$; for initial magnetization $M(0) \simeq 0$ these states are well established for $0.60 \leqslant U \leqslant 0.73$. The results for both conditions are compared in the inset, where the duration $t_{\rm QSS}$ is conveniently represented in a log-log plot, showing that close to U_c the data for both initial conditions coincide. From now on, we restrict our analysis to the initial condition of magnetization $M(0) \simeq 0$.

Similar plots are exhibited in Fig. 2(a) where the kinetic temperature $T(t)$ is represented versus time, for the α-XY model with $\alpha/d = 0.9$, and lattice dimensions $d = 1, 2, 3$. Several values of $U < U_c$ are considered, and one notices that the duration $t_{\rm QSS}$ increases with U (d fixed), as well as with d (U fixed). We call the attention to the particular growth with U, as U_c is approached from below; in fact, the insets of both Figs. 1 and 2(a) indicate a powerlike divergence as $U \to U_c$,

$$t_{\rm QSS} \propto (U_c - U)^{-\xi} \quad (U_c = 3/4,\ \xi \simeq 1.67), \tag{8}$$

typical of a critical phenomenon [1]. The inset of Fig. 2(a) yields a contribution to the proportionality factor, d^ρ ($\rho = 0.31$), introduced in Ref. [33], which becomes necessary as α/d approaches the short-range regime, so that $\rho = 0$ ($\alpha/d \leqslant 0.7$) and $\rho = 0.31$ ($\alpha/d = 0.8, 0.9$). In Fig. 2(b) we represent typical curves of $T(t)$ [chosen from Fig. 2(a)], for U approaching U_c (from below), in conveniently defined dimensionless variables, i.e., $T_{\rm scaled}(t) = [T(t) -$

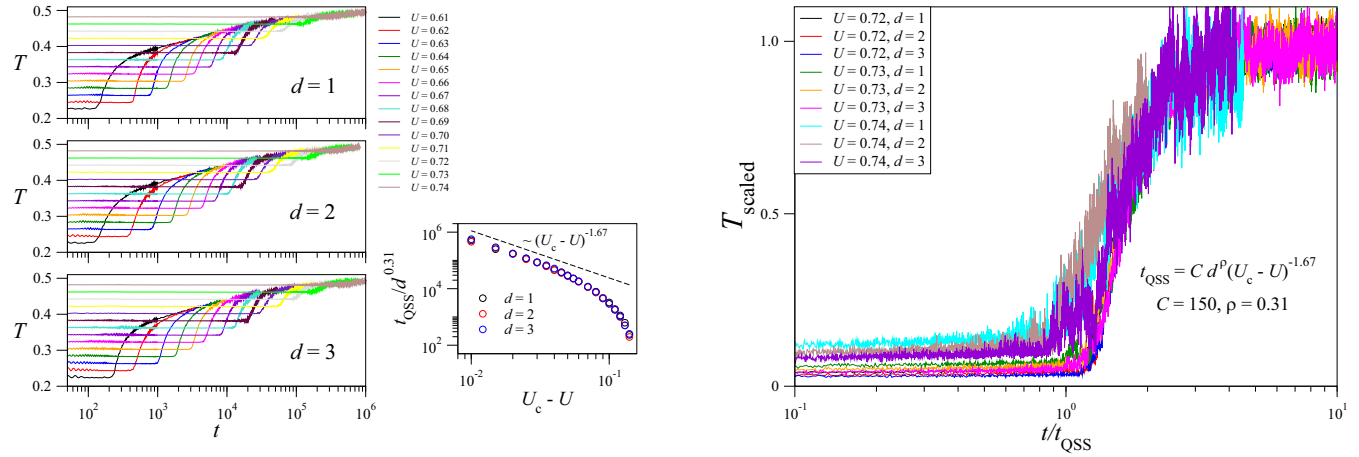

(a) (b)

FIG. 2. (a) The kinetic temperature $T(t)$ of Eq. (5) is represented vs time (in logarithmic scale), for the α-XY model with $\alpha/d = 0.9$, $N = 262\,144$ ($d = 1, 2, 3$), typical values of $U < U_c$ ($U_c = 3/4$), considering the initial condition $M(0) \simeq 0$. Notice that the duration $t_{\rm QSS}$ increases with U (d fixed) and d (U fixed). In the inset we represent $t_{\rm QSS}$ (properly rescaled) vs $(U_c - U)$ in a log-log plot showing a data collapse. (b) Typical curves as $U \to U_c$ [from (a)] are exhibited in convenient dimensionless variables in a linear-log representation; the collapse for three different values of U ($d = 1, 2, 3$) indicates the appropriateness of the scaling $t_{\rm QSS} = C d^\rho (U_c - U)^{-1.67}$ (see text).

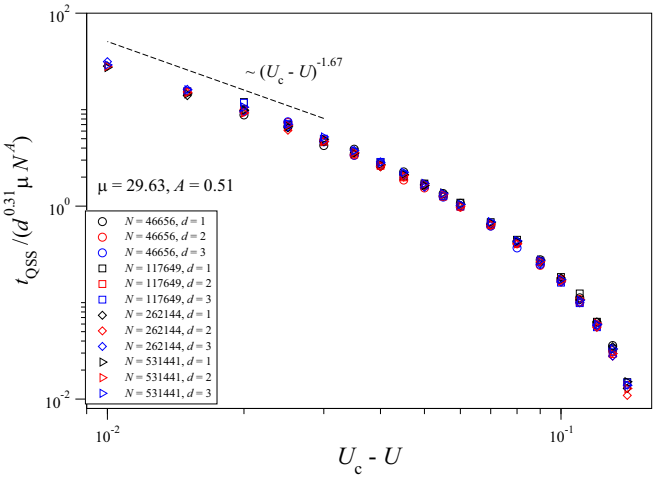

FIG. 3. Data for the duration $t_{\rm QSS}$ of Fig. 2(a) ($N = 262\,144$ and $\alpha/d = 0.9$) are exhibited in conveniently rescaled variables vs $(U_c - U)$ in a log-log plot; results from similar analyses, with other values of N ($N = 46\,656$, 117 649, and 531 441) are also presented. Following Ref. [33], a collapse of all data is verified, where the two fitting parameters μ and A depend on the ratio α/d, and for the present case, $\mu(0.9) = 29.63$ and $A(0.9) = 0.51$. A good agreement of the data with the scaling of Eq. (8) is verified as $U \to U_c$.

$T_{\rm QSS}(t)]/[T_{\rm BG}(t) - T_{\rm QSS}(t)]$ vs $t/t_{\rm QSS}$, where $T_{\rm QSS}(t)$ and $T_{\rm BG}(t)$ represent, respectively, the kinetic temperature at the QSS and BG temperature at the upper plateau; in the abscissa, $t_{\rm QSS} \sim C d^{\rho}(U_c - U)^{-1.67}$, where C will be identified below. Using these variables, a reasonably good collapse of nine curves from Fig. 2(a) ($U = 0.72, 0.73, 0.74$, for $d = 1, 2, 3$) is observed.

The analysis of Fig. 2(a) was repeated for several values of N, yielding the data presented in Fig. 3, where we plot the duration $t_{\rm QSS}$ (conveniently rescaled) versus $(U_c - U)$, in a log-log plot. The data collapse extends the results obtained previously for $U = 0.69$, $d = 1, 2, 3$, and fixed values of α/d [cf. Eq. (3.1) in Ref. [33]], to a broader energy range,

$$t_{\rm QSS} = d^{\rho}\mu(\alpha/d)N^{A(\alpha/d)}\,\epsilon^{-\xi}, \tag{9}$$

where $\epsilon \equiv (U_c - U)/(U_c - 0.69)$; the fitting parameters $\mu(\alpha/d)$ and $A(\alpha/d)$ are given in Fig. 3 for the case $\alpha/d = 0.9$; to define ϵ we refer to $U = 0.69$ because this value is frequently used in the literature since it yields, for the present model, the largest discrepancy between $T_{\rm QSS}$ and $T_{\rm BG}$. It is important to mention that, considering the sizes investigated (typically varying by a factor of 10 in Fig. 3), the exponent $\xi \simeq 1.67$ did not significantly change, indicating that our simulations have attained sufficiently large N values.

In Fig. 4(a) we exhibit data of the duration $t_{\rm QSS}$, obtained from simulations of $N = 46\,656$ rotators, versus $(U_c - U)$, in a log-log representation. Different values of α/d were considered, i.e., $\alpha/d = 0.5, 0.6, 0.7, 0.8, 0.9$, and, for completeness, we include the results for the HMF model (limit $\alpha = 0$) of Fig. 1. As $U \to U_c$, all cases show a good agreement with the scaling of Eq. (8); in the inset, using the proposal of Ref. [33], one observes a collapse of all data for different values of α/d. The results of Fig. 4(a) extend the energy range of those obtained previously for $U = 0.69$, $d = 1, 2, 3$, and fixed values of N [cf. Eq. (3.2) in Ref. [33]], yielding

$$t_{\rm QSS} = d^{\rho}\nu(N)\exp[-B(N)(\alpha/d)^2]\epsilon^{-\xi}, \tag{10}$$

where the two N-dependent fitting parameters present the values $\nu(N) = 1.7 \times 10^7$ and $B(N) = 9.52$. We emphasize that the results of Fig. 4(a) indicate universality of the exponent ξ with respect to α/d, i.e., $\xi \simeq 1.67$ for all $0 \leqslant \alpha/d \leqslant 1$. In Fig. 4(b) the data of Fig. 3 (several values of N, $\alpha/d = 0.9$) are plotted together with those of Fig. 4(a) ($N = 46\,656$ and various α/d); the collapse shows a good agreement of all data with the scaling of Eq. (8), for $U \to U_c$. Consequently, the factor $C = 150$ of Fig. 2(b) [valid for $N = 262\,144$, $\alpha/d = 0.9$ ($d = 1, 2, 3$)] is compatible with those that appear either in Eq. (9), or in Eq. (10), within a 4%

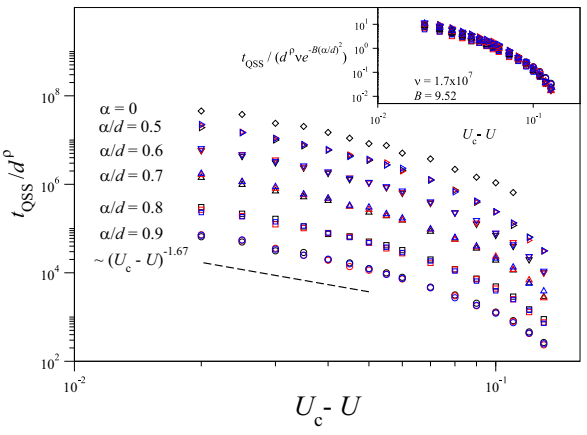

(a)

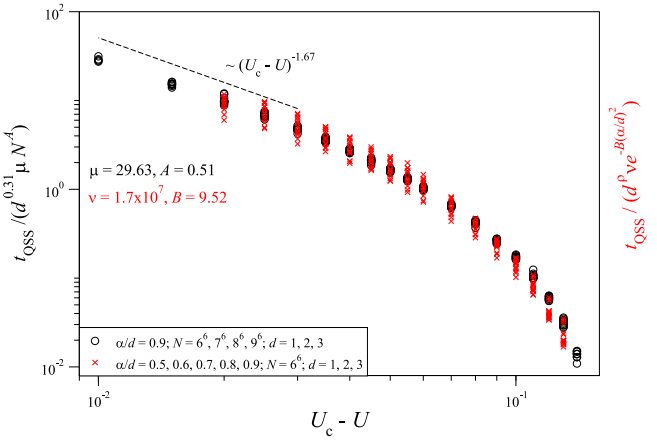

(b)

FIG. 4. (a) Data for the duration $t_{\rm QSS}$ (conveniently rescaled) is represented vs $(U_c - U)$ in a log-log plot, considering $N = 46\,656$, several values of α/d ($\alpha/d = 0.5, 0.6, 0.7, 0.8$, and 0.9), and dimensions $d = 1$, 2, and 3; for completeness, the $\alpha = 0$ results of Fig. 1 are also shown. In the inset, using the proposal of Ref. [33], one observes a data collapse. (b) Data of the inset in (a) (red crosses) are plotted together with those of Fig. 3 (open black circles), thus exhibiting that Eqs. (9) and (10) are numerically equivalent for the entire range of parameters used here.

discrepancy. In fact, variations in C lead to translations of the whole group of curves in Fig. 2(b), so that by adjusting appropriately this factor it is possible to centralize all curves around $t/t_{\rm QSS} = 1$.

IV. CONCLUSIONS

To conclude, we have found a critical phenomenon associated with the duration $t_{\rm QSS}$ of the quasistationary states that occur in the d-dimensional classical inertial α-XY model. These states emerge throughout the whole long-range interaction regime ($0 \leqslant \alpha/d \leqslant 1$), for an average energy per rotator $U < U_c$, where $U_c = 3/4$ represents the critical energy associated with the ferromagnetic-paramagnetic phase transition. Hence, the quasistationary states appear throughout the whole ferromagnetic phase, but not in the paramagnetic one. We have shown that, contrary to the belief that these states simply disappear in the limit $U \to U_c$ (from below), they actually go through an interesting critical phenomenon following $t_{\rm QSS} \propto (U_c - U)^{-\xi}$, where the critical exponent $\xi \simeq 5/3$ is universal along the whole long-range interaction regime ($0 \leqslant \alpha/d \leqslant 1$), for $d = 1, 2, 3$, and arbitrary large values of N. Usually, critical phenomena occur in highly connected many-particle systems (essentially, in the limit $N \to \infty$), for a sufficiently low temperature (or equivalently, low internal energy per particle), which represent some of the requirements for the existence of the quasistationary states in the d-dimensional classical inertial α-XY model. Consequently, the above-mentioned critical effect is associated with these nonequilibrium states, present throughout the whole ferromagnetic phase. The divergence of $t_{\rm QSS}$ in the limit $U \to U_c$ (from below) should be influenced by the strong correlations that are expected to arise (also in quasistationary states), as one approaches the well-established equilibrium phase transition between the ferromagnetic and paramagnetic states. Further properties, such as the existence of an associated diverging correlation length, in these out-of-equilibrium states, are the object of future investigations. This dynamical critical phenomenon should occur also in other long-range-interaction models (e.g., with the Heisenberg model symmetry), leading to a better understanding of their corresponding long-living non-Boltzmannian states.

ACKNOWLEDGMENTS

We have benefited from partial financial support by the Brazilian agencies CNPq and Faperj, and Universidad Politécnica de Madrid.

[1] H. E. Stanley, *Introduction to Phase Transitions and Critical Phenomena* (Oxford University Press, Oxford, UK, 1971).
[2] R. K. Pathria and P. D. Beale, *Statistical Mechanics*, 3rd ed. (Elsevier, Amsterdam, 2011).
[3] P. Bak, *How Nature Works: The Science of Self-Organized Criticality* (Copernicus, New York, 1996).
[4] M. Henkel, H. Hinrichsen, and S. Lübeck, *Non-Equilibrium Phase Transitions*, Vol. 1 (Springer, Netherlands, 2008).
[5] M. Henkel and M. Pleimling, *Non-Equilibrium Phase Transitions*, Vol. 2 (Springer, Netherlands, 2010).
[6] C. Anteneodo and C. Tsallis, Breakdown of Exponential Sensitivity to Initial Conditions: Role of the Range of Interactions, Phys. Rev. Lett. **80**, 5313 (1998).
[7] M. Antoni and S. Ruffo, Clustering and relaxation in Hamiltonian long-range dynamics, Phys. Rev. E **52**, 2361 (1995).
[8] P. Jund, S. G. Kim, and C. Tsallis, Crossover from extensive to nonextensive behavior driven by long-range interactions, Phys. Rev. B **52**, 50 (1995).
[9] C. Tsallis, Nonextensive thermostatistics and fractals, Fractals **3**, 541 (1995).
[10] M.-C. Firpo, Analytic estimation of the Lyapunov exponent in a mean-field model undergoing a phase transition, Phys. Rev. E **57**, 6599 (1998).
[11] V. Latora, A. Rapisarda, and S. Ruffo, Lyapunov Instability and Finite Size Effects in a System with Long-Range Forces, Phys. Rev. Lett. **80**, 692 (1998).
[12] V. Latora, A. Rapisarda, and S. Ruffo, Superdiffusion and Out-of-Equilibrium Chaotic Dynamics with Many Degrees of Freedom, Phys. Rev. Lett. **83**, 2104 (1999).
[13] V. Latora, A. Rapisarda, and C. Tsallis, Non-Gaussian equilibrium in a long-range Hamiltonian system, Phys. Rev. E **64**, 056134 (2001).
[14] J. Barré, F. Bouchet, T. Dauxois, and S. Ruffo, Out-of-Equilibrium States and Statistical Equilibria of an Effective Dynamics in a System with Long-Range Interactions, Phys. Rev. Lett. **89**, 110601 (2002).
[15] A. Pluchino, V. Latora, and A. Rapisarda, Metastable states, anomalous distributions and correlations in the HMF model, Physica D **193**, 315 (2004).
[16] A. Pluchino, V. Latora, and A. Rapisarda, Glassy phase in the Hamiltonian mean-field model, Phys. Rev. E **69**, 056113 (2004).
[17] L. G. Moyano and C. Anteneodo, Diffusive anomalies in a long-range Hamiltonian system, Phys. Rev. E **74**, 021118 (2006).
[18] A. Pluchino, A. Rapisarda, and C. Tsallis, Nonergodicity and central-limit behavior for long-range Hamiltonians, Europhys. Lett. **80**, 26002 (2007).
[19] A. Pluchino, A. Rapisarda, and C. Tsallis, A closer look at the indications of q-generalized Central Limit Theorem behavior in quasi-stationary states of the HMF model, Physica A **387**, 3121 (2008).
[20] A. Campa, P. H. Chavanis, A. Giansanti, and G. Morelli, Dynamical phase transitions in long-range Hamiltonian systems and Tsallis distributions with a time-dependent index, Phys. Rev. E **78**, 040102(R) (2008).
[21] A. Campa, T. Dauxois, and S. Ruffo, Statistical mechanics and dynamics of solvable models with long-range interactions, Phys. Rep. **480**, 57 (2009).
[22] A. Campa, T. Dauxois, D. Fanelli, and S. Ruffo, *Physics of Long-Range Interacting Systems* (Oxford University Press, Oxford, UK, 2014).
[23] A. R. Plastino, E. M. F. Curado, F. D. Nobre, and C. Tsallis, From the nonlinear Fokker-Planck to the Vlasov description and

back: Confined interacting particles with drag, Phys. Rev. E **97**, 022120 (2018).

[24] G. Giachetti, A. Santini, and L. Casetti, Coarse-grained collisionless dynamics with long-range interactions, Phys. Rev. Research **2**, 023379 (2020).

[25] C. Tsallis, *Introduction to Nonextensive Statistical Mechanics—Approaching a Complex World* (Springer, New York, 2009).

[26] C. Tsallis, Beyond Boltzmann-Gibbs-Shannon in physics and elsewhere, Entropy **21**, 696 (2019).

[27] C. Tsallis, Possible generalization of Boltzmann-Gibbs statistics, J. Stat. Phys. **52**, 479 (1988).

[28] A. Campa, A. Giansanti, and D. Moroni, Canonical solution of a system of long-range interacting rotators on a lattice, Phys. Rev. E **62**, 303 (2000).

[29] F. Tamarit and C. Anteneodo, Rotators with Long-Range Interactions: Connection with the Mean-Field Approximation, Phys. Rev. Lett. **84**, 208 (2000).

[30] A. Campa, A. Giansanti, D. Moroni, and C. Tsallis, Classical spin systems with long-range interactions: Universal reduction of mixing, Phys. Lett. A **286**, 251 (2001).

[31] L. J. L. Cirto, V. R. V. Assis, and C. Tsallis, Influence of the interaction range on the thermostatistics of a classical many-body system, Physica A **393**, 286 (2014).

[32] L. J. L. Cirto, A. Rodríguez, F. D. Nobre, and C. Tsallis, Validity and failure of the Boltzmann weight, Europhys. Lett. **123**, 30003 (2018).

[33] A. Rodríguez, F. D. Nobre, and C. Tsallis, Quasi-stationary-state duration in the classical d-dimensional long-range inertial XY ferromagnet, Phys. Rev. E **103**, 042110 (2021).

[34] L. J. L. Cirto, L. S. Lima, and F. D. Nobre, Controlling the range of interactions in the classical inertial ferromagnetic Heisenberg model: analysis of metastable states, J. Stat. Mech: Theory Exp. (2015) P04012.

[35] A. Rodríguez, F. D. Nobre, and C. Tsallis, d-dimensional classical Heisenberg model with arbitrarily-ranged interactions: Lyapunov exponents and distributions of momenta and energies, Entropy **21**, 31 (2019).

[36] A. Rodríguez, F. D. Nobre, and C. Tsallis, Quasi-stationary-state duration in d-dimensional long-range model, Phys. Rev. Research **2**, 023153 (2020).

[37] C. G. Antonopoulos and H. Christodoulidi, Weak chaos detection in the Fermi-Pasta-Ulam-α system using q-Gaussian statistics, Int. J. Bifurcation Chaos Appl. Sci. Eng. **21**, 2285 (2011).

[38] H. Christodoulidi, C. Tsallis, and T. Bountis, Fermi-Pasta-Ulam model with long-range interactions: Dynamics and thermostatistics, Europhys. Lett. **108**, 40006 (2014).

[39] H. Christodoulidi, T. Bountis, C. Tsallis, and L. Drossos, Dynamics and statistics of the Fermi-Pasta-Ulam β-model with different ranges of particle interactions, J. Stat. Mech.: Theory Exp. (2016) 123206.

[40] D. Bagchi and C. Tsallis, Sensitivity to initial conditions of a d-dimensional long-range interacting quartic Fermi-Pasta-Ulam model: Universal scaling, Phys. Rev. E **93**, 062213 (2016).

[41] D. Bagchi and C. Tsallis, Fermi-Pasta-Ulam-Tsingou problems: Passage from Boltzmann to q-statistics, Physica A **491**, 869 (2018).

[42] H. Yoshida, Construction of higher order symplectic integrators, Phys. Lett. A **150**, 262 (1990).